# Concrete-to-concrete connections for modularly reused RC components – an experimental study on separation methods

David Sanio*[1][0000-0002-2507-3578], Sven Simon[2], Daniel Balzani[3][0000-0002-1422-4262] and Peter Mark[1][0000-0003-1812-2148]

[1] Institute of Concrete Structures, Ruhr University Bochum, Germany
[2] Department of Computational Imaging Systems, University of Stuttgart, Germany
[3] Chair of Continuum Mechanics, Ruhr University Bochum, Germany
*david.sanio@rub.de

**Abstract.** For the reuse of RC structures, structural components like columns or beams are extracted from monolithic buildings to serve as reused modules for newly assembled structures in a sense of construction kits. The scope of this study is an experimental investigation of the newly formed concrete-to-concrete connections between the modules that might transfer compression and shear.
The load-bearing capacity of the connections are predominated by the characteristics of the module's edge. For RC, inaccuracies of the surface, damages from separation as well as the stress inhomogeneities due to the cut off reinforcement that ends up bluntly have to be taken into account.

The paper presents an experimental campaign on the three named aspects. 16 RC beams with a rectangular cross section are cut by sawing, waterjet cutting or hammering and then tested under centric or eccentric compression. Concrete-to-concrete and concrete-to-steel connections are tested. Process parameters like the cutting speed, cutting depth and post-treatment by grinding are considered and varied. CT and laser scans quantify the micro damage as well as the surfaces' flatness that arise from the separation. The results show that precise sawing ensures a load-bearing capacity similar to a fully plastic activation of all rebars and concrete areas. On the contrary, rough cuttings significantly diminish ultimate loads. The results are discussed with respect to surface qualities and inevitable micro damages and referenced to newly built RC sections.

**Keywords:** Reuse, Concrete-to-concrete connections, separation, cutting, CT.

## 1 Introduction

To ensure sustainability, greenhouse gas emissions and resource consumption in construction must be reduced. One approach is the reuse of structural components [1], as it is under research for new structures [2,3]. In order to make the best possible use of the existing anthropogenic material stock [4], reuse is already practiced in steel construction [5] and under development for concrete components: both for prefabricated components with predefined joints [6,7] and for cast-in-place concrete [7,8].

The reuse of cast-in-place concrete requires the monolithic structure to be separated into modules (Fig. 1a), which are then reassembled to form new load-bearing structures (Fig. 1c). This requires new connections of the modules. The load-bearing capacity of the undesigned component edges with cut off reinforcement (Fig. 1b) significantly determines the load-bearing capacity of the new connections.

The paper shows the results of an experimental study of the load-bearing capacity of new concrete connections under compression with and without eccentricity. Different separation methods that introduce damage into the module's edge [9,10] are considered and their influence on the load-bearing capacity is investigated.

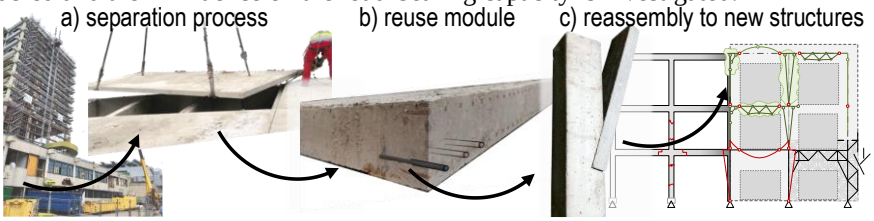


**Fig. 1.** Basic idea of the modular reuse: From the separation of entire modules from existing monolithic structures to the reassembly of new structures.

## 2 Experimental program

### *2.1 Specimens and separation methods*

The 16 test specimens (Table 1) investigated, are concrete prisms (dimensions $l$ x $w$ x $h$ = ~ 230 x 80 x 80 [mm]) with a centric rebar Ø = 16 mm (reinforcement ratio $\rho$ = 0.031, $f_y$ = 500 N/mm²). The concrete used corresponds to a class of strength C30/37 with $f_{cm}$ = 35.4 N/mm², $f_{cm,cube}$ = 42.7 N/mm² and $E_{cm}$ = 26146 N/mm².

Four test specimens each were taken from one concrete beam (4 beams in total, $l$ = 1.00 m) by varying the separation method. The separation methods used are a concrete saw (Fig. 2a), waterjet (WJ) (Fig. 2b), hydraulic hammer (Fig. 2c) and hydraulic crusher (Fig. 2d). The cut surfaces of individual specimens are shown in Fig. 3.


**Fig. 2.** Separation process by a) sawing, b) waterjet, c) hydraulic hammering and d) crushing.

The process parameters of the saw and the WJ were varied. The saw cut was alternatively multi-staged with cutting depths of 1 cm, in one stage (8 cm) and combined with twisting the specimen during sawing. One surface was grinded (B1-a).

In the case of WJ, one cut was made with a steel sheet underneath to reduce the concrete break-out at the bottom (B3-a & b). The second cut was made with a steel plate ($t$ = 10 mm) on top to reduce the accuracy of the jet stream (B3-c & d).

**Table 1.** Separation methods of the concrete specimens and experimental parameters.

| Spec. | Separation method left & right surf. | | Description | Bearings | Ecc. *e/h* |
|---|---|---|---|---|---|
| B1-a | saw, multi-stage + grinded** | saw, multi-stage** | reference | steel - steel | 0 |
| B1-b | saw, multi-stage** | saw, multi-stage | reference | steel – concrete | 0 |
| B1-c | saw, multi-stage | saw, multi-stage** | reference | steel – steel | 0 |
| B1-d | saw, multi-stage | saw, multi-stage | reference eccentric | steel – steel | 0.125 |
| B2-a | saw, multi-stage** | saw, multi-stage** | precise sawing | steel – steel | 0 |
| B2-b | saw, multi-stage | saw, 1 stage** | rough sawing* | - | - |
| B2-c | saw, 1 stage | saw, twisted** | rough & skewed sawing | steel – steel | 0 |
| B2-d | saw, twisted** | saw, multi-stage** | skewed sawing | steel – concrete | 0 |
| B3-a | saw, multi-stage | WJ, on steel | precise waterjet | steel – concrete | 0 |
| B3-b | WJ, on steel | saw, multi-stage | precise waterjet | steel – concrete | 0.125 |
| B3-c | saw, multi-stage | WJ, through steel | rough waterjet* | - | - |
| B3-d | WJ, through steel | saw, multi-stage | rough waterjet | steel – concrete | 0 |
| B4-a | saw, multi-stage | Hydraulic hammer | hammering* | - | - |
| B4-b | Hydraulic hammer | saw, multi-stage | hammering | - | - |
| B4-c | saw, multi-stage | Hydraulic crusher | crushing | - | - |
| B4-d | Hydraulic crusher | saw, multi-stage | crushing | - | - |

* for CT-scans ** concrete break-out

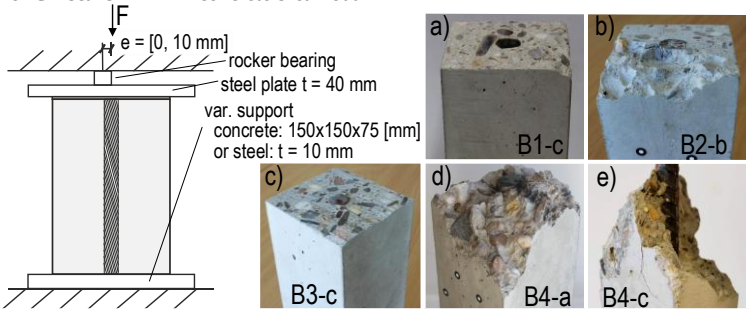


**Fig. 3.** Test setup (left) and cut surfaces with variable separation methods (right, a-e).

### *2.2 Mechanical tests: setup and experimental procedure*

The specimens were tested to failure in centric and eccentric compression tests (Fig. 3) with displacement control. The upper support was realized by a steel plate. The lower support was alternatively a concrete block or a steel plate. Eccentric loading with $e$ = 10 mm was implemented using a rocker bearing.

10 specimens were mechanically tested. 3 were used for CT-scans. The macroscopic damage on those specimens that were separated by hammering and crushing was too severe to allow mechanical testing. The rebar protruded far out, and it was not possible to apply loads on the concrete surface without refurbishment.

### *2.3 3D- and CT-scans*

3D-Scans allow the characterization of the specimen's geometry and the flatness of the cut surface. A stereo camera system GOM Atos Compact Scan 8M was used here that generates a dense cloud of points with around $7.5 \cdot 10^5$ for each specimen. This comes from around 30 scans from different angles by rotating the specimen. Common

points, identified in each image from marked points, help to generate a 3D model of the specimen by stereo photogrammetric methods combined with a structured blue light [10]. The measurement uncertainty is around ±0.01 mm.

Inner damage like cracking and debonding can be detected by computer tomography (CT). 3 specimens (B2-b, B3-c and B4-a) were scanned by CT. The result is a large number of slices that are processed into a 3D voxel image of the specimen.

# 3 Results

## *3.1 Mechanical tests*

The results from the compression tests are shown as force over displacement in Fig. 4a for the centric test and steel support, in Fig. 4b for the concrete support and in Fig. 4c for eccentric loading. The corresponding results for $e = 0$ are given for comparison. The theoretical load-bearing capacities acc. to Sect. 4.1 are given as dashed grey lines.

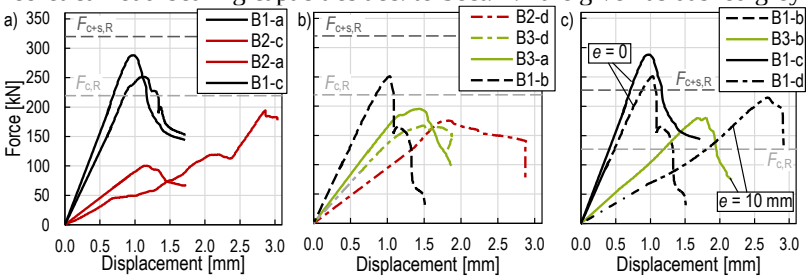


**Fig. 4.** Experimental results from compression tests for a) steel support, b) concrete support and c) with and without eccentricity

In all tests, a compression failure of the concrete was observed by longitudinal cracks in the concrete from splitting, as it was expected [12,13]. For the concrete support, also a bond failure was observed by pushing the rebar out of the concrete. The butt end rebar pressed into the concrete block and led to partial block splitting.

## *3.2 Surface flatness from 3D-scans*

The surface flatness was determined by 3D-scans [14]. The root-mean-square flatness deviation $\Delta F_{rms}$ acc. to ISO 12781-1:2011 serves as a measure of unevenness. It is calculated with Eq. 1 from the local flatness deviation $\Delta F_l$ and $A$ as the surface area.

$$\Delta F_{rms} = (1/A \int_A \Delta F_l^2 \, dA)^{½} \quad (1)$$

Fig. 5 shows the results of 3 samples. All results are summarized in Fig. 7. The lowest flatness deviation is achieved by sawing (Fig. 5a with $\Delta F_{rms,B1\text{-}d} = 0.265$ mm). In case of concrete break-out from sawing, there are locally limited areas with large flatness deviations (Fig. 5b, $\Delta F_{rms,B2\text{-}a} = 0.800$ mm) and no contact to the loading plate in testing. This local effect significantly increases $\Delta F_{rms}$ depending on the break-out size. With WJ, the surface shows slight wavelike variations in flatness (Fig. 5c,

$\Delta F_{rms,B3\text{-}a}$ = 0.438 mm). However, this is greater than with precision sawing.

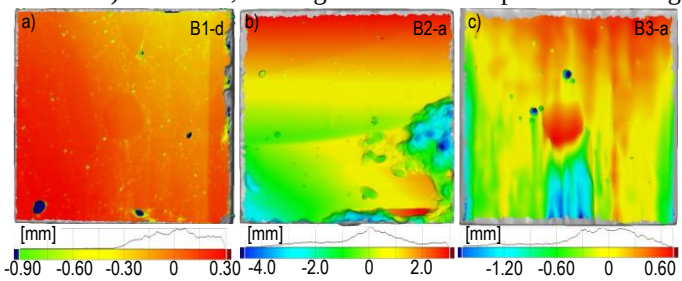


**Fig. 5.** Surface profiles from 3D-scans with corresponding histograms of local flatness deviations for a) B1-d precise sawing, b) B2-a precise sawing with breakout and c) B3-a WJ

### *3.3 CT-scans*

The CT-scans show significant cracks in B4-a (Fig. 6a), which can be found up to a depth of >10 cm from the cut surface. The sawn specimen B2-b indicates no cracks (Fig. 6b), but concrete break-out on the surface and slight detachment of the rebar from the concrete at the cut edge. WJ (B3-c in Fig. 6c) leads to no cracks, but a cavity formation in the direction of the waterjet under the reinforcing bar.

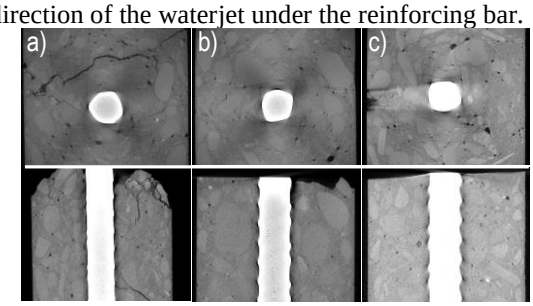


**Fig. 6.** Scan result for as horizontal (top) and vertical sections (bottom) through the volume

Moreover, the CT slices in Fig. 6 show dark regions between concrete and reinforcement all over the entire bond length which do not necessarily correspond to damage. Instead, imaging artifacts may be the cause. In particular, metals lead to strong artifacts that depend on both the geometry of the metal object and the X-ray absorption coefficient. The reason for the artifacts on metals is, on the one hand, the fact that X-ray tubes generate photons with different energies and, on the other hand, the X-ray absorption, which represents the grey value in the CT volume and is strongly energy-dependent. This results in so-called beam-hardening artifacts that lead to a higher grey value at the edges of the metals and a lower grey value in the middle of the metal structure. Reinforcement is strongly affected by these artifacts at the metal-concrete interface, so that further research is required to identify real bond damage.

# 4 Discussion

## *4.1 Theoretical load bearing capacity*

The theoretical load bearing capacity of the specimens serves to evaluate bearing effects from the separation. It is calculated separately for concrete $F_{c,R}$ and steel $F_{s,R}$ (Eq. 3) and then combined to $F_{c+s.R}$ (Eq. 2). Doing so, simplified approaches are assumed. Under compression, the full plastic bearing load is determined from the full plastic compressive strength of concrete $f_c$ and steel $f_y$ and the corresponding cross-sectional area (Eq. 3). For the concrete, the net cross-sectional area $A_{c,n}$ is considered, for the steel the area of the rebar $A_s$.

$$F_{c+s,R}(e) = F_{c,R} + F_{s,R} \tag{2}$$

$$F_{c,R} = f_c\, A_{c,n} \quad \text{and} \quad F_{s,R} = f_y\, A_s \tag{3}$$

For compression and compression with bending at low load eccentricity within the first core width ($e/h < 1/6$) of the cross-section, a linear stress distribution in the cross-section is assumed. Therefore, the load-bearing capacity of the concrete (Eq. 4) follows from the stress equation with $W_{y,n}$ as the net section modulus of the concrete.

$$F_{c,R}(e) = f_c\, W_{y,n}\, A_{c,n} / (W_{y,n} + e\, A_{c,n}) \tag{4}$$

For simplicity, the full centric load-bearing capacity of the rebar is assumed and $F_{c+s,R}(e)$ follows from Eq. 2. For the specimens (see Sect. 2.1), this results in a theoretical full plastic centric load-bearing capacity $F_{c+s,R}(e = 0) = 219.4 + 100.5 = 320.0$ kN and with eccentricity $F_{c+s,R}(e = 10\text{ mm}) = 126.9 + 100.5 = 256.3$ kN.

## *4.2 Impact of the separation method*

Hammering caused macroscopic damage with cracks down to a depth of at least 10 cm in our experiments. This area would need to be removed or refurbished for reuse. Crushing causes similarly severe damage (Fig. 3e). B4-d was split longitudinally during separation. During sawing, edge break-out occasionally occurs, which can be larger depending on the process parameters. However, small break-out also occurs during precise sawing (B1-c). Micro-cracking as found in [10], was not observed here. In case of the WJ, there is no significant impact from cutting with the steel plate on top and below. In all samples, a cavity appears in the concrete underneath the rebar, which is attributed to deflection or dispersion of the waterjet by the steel.

The comparison with the theoretical load bearing capacity shows that $F_{c,R}$ is exceeded for the centrally loaded specimens of reference series B1 and 0.78 to 0.90 of $F_{c+s,R}$ is achieved. The B1-d eccentrically loaded achieves 0.93 $F_{c+s,R}(e = 10\text{ mm})$. By varying the process parameters of the saw (faster, higher cutting depth), the load bearing capacity drops significantly and only reaches 0.45 to 0.89 $F_{c,R}$ and 0.31 to 0.61 $F_{c+s,R}$, respectively. This is associated with larger concrete break-outs. The impact of the WJ is similar with a uniform load bearing capacity of 0.76 to 0.89 $F_{c,R}$ and 0.52 to 0.61 $F_{c+s,R}$, respectively. Only the eccentrically loaded sample exceeds the bearing

capacity of the concrete and reaches 0.79 $F_{c+s,R}(e = 10\ \text{mm})$.

An impact of the eccentricity can only be seen in the reference series B1. There, the eccentrically loaded sample B1-d drops by approx. 18 % compared to the mean value from B1-a to c. However, the theoretical load reduction due to the eccentricity is 28 % = [1 - $F_{c+s,R}(e = 10\ \text{mm})$ / $F_{c+s,R}(e = 0)$] that is not achieved. It needs further investigations to clarify whether this is due to the small sample size or other relevant influencing factors. In contrast, no influence of the eccentricity is evident for WJ. This can be attributed to the fact that the influence of the flatness deviation is neutralized here with an accompanying reduced contact area.

### *4.3 Impact of surface flatness*

A comparison of the surface flatness to the relative maximum test load, related to $F_{c+s,R}(e)$ is given in Fig. 7. In the literature, a significant impact of the surface can be found depending on the precision of molds [15,16]. For the test with steel support on both sides, a linear trend is recognizable (triangles in Fig. 7). The max. test load decreases with increasing flatness deviations. In contrast, no trend is detectable for the test specimens with lower concrete support, which show a random variation.

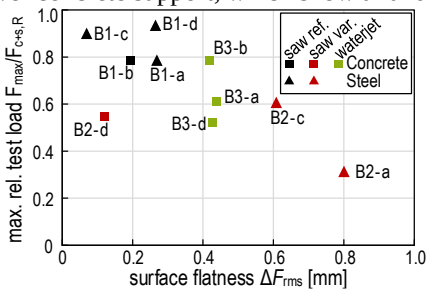


**Fig. 7.** Maximum relative test load over the surface flatness deviation with differentiation between separation method and lower bearing ($e = 0$ and $e = 10$ mm combined)

## 5 Conclusions

The following conclusions can be drawn based on the experimental study:

- Rough cutting methods (hammer, crusher) cause substantial damage to the edge even at considerable depths from the cut surface. Cracks have been found to depths of > 10 cm. This requires refurbishment of the edge for reuse.
- With precise separation methods like waterjet or sawing, no cracks were found in the concrete, although they can be expected from sawing [9,10]. However, sawing causes edge breakage of the concrete and slight detachment of the reinforcement from the concrete. Further investigations with varying process parameters (sawing speed, cutting depth, material properties, geometry) and at a higher resolution are required. Moreover, protection of the cut specimen at its borders seems reasonable.
- The load-bearing capacity of the connection decreases with increasing flatness deviation. The correlation is lower with the softer concrete support, whereby the failure

also occurs in the bond between concrete and steel.
- The impact of localized edge break-out is dominant in single cases. As it is primarily expected in the concrete cover, the influence is expected to be reduced for larger surfaces and for areas surrounded by stirrup reinforcements.
- Further investigations are required to characterize the depth of damage caused by rough separation methods more precisely. At the same time, the required flatness and appropriate refurbishment methods and areas must be investigated in detail.

The study is a first step towards a full understanding of the complex phenomena observed in the boundary layers of extracted modules resulting from cutting processes. Computational modeling and analysis, including detailed mesostructural models, will allow quantification of the graded properties resulting from damage in the concrete matrix and at the reinforcement-concrete interface. Based on this, optimized decisions can be made regarding the processing of the interfaces for tailored joint solutions.

## References


1. Hradil P et al. (2014) Re-use of structural elements. Environmentally efficient recovery of building components. VTT Technology T200. VTT Technical Research Centre, Finland.
2. Bertin I et al. (2019) Construction, deconstruction, reuse of the structural elements: the circular economy to reach zero carbon. IOP Conf Ser.: Earth Environ Sci 323:12020.
3. Ebert S et al. (2020) Model for the recyclability of building components. Bautechnik 97:14-25
4. Rose CM, Stegemann JA (2019) Characterising existing buildings as material banks (E-BAMB) to enable component reuse. Eng. Sust. 172:129–140. doi: 10.1680/jensu.17.00074
5. Fivet C (2022) Steel, a material to reuse. Stahlbau 91:268–273.
6. Huuhka S et al. (2015) Reusing concrete panels from buildings for building. Resources, Conservation and Recycling 101:105–121. doi: 10.1016/j.resconrec.2015.05.017
7. Küpfer C et al. (2023) Reuse of concrete components in new construction projects: Critical review of 77 circular precedents. Journal of Cleaner Production 383:135235.
8. Roth L, Eklund M (2000) Environmental analysis of reuse of cast-in-situ concrete in the building sector. Towards Sustainability in the Built Environment 2000:234–243
9. Zhang Z et al. (2020) A laboratory investigation of cutting damage to the steel-concrete interface. Cement and Concrete Research 138:106229.
10. Kustermann A (2005) Einflüsse auf die Bildung von Mikrorissen im Betongefüge. PhD-Thesis, University of the Bundeswehr Munich (German)
11. Barbero BR, Ureta ES (2011) Comparative study of different digitization techniques and their accuracy. Computer-Aided Design 43:188–206. doi: 10.1016/j.cad.2010.11.005
12. Schmidt-Thrö G et al. (2018) Experimental investigations of partial loading capacity with plane load distribution. Beton- und Stahlbetonbau 113:115–126.
13. Plückelmann S et al. (2019) Bearable local stress of high-strength steel fiber reinforced concrete. Beton- und Stahlbetonbau 114:653–662
14. Santos PM, Júlio EN (2013) A state-of-the-art review on roughness quantification methods for concrete surfaces. Construction and Building Materials 38:912–923
15. Richardson DN (1991) Review of Variables that Influence Measured Concrete Compressive Strength. J Mater Civ Eng 3:95–112. doi: 10.1061/(ASCE)0899-1561(1991)3:2(95)
16. Ahmadi B et al. (2022) Investigation the Effect of Perpendicularity and Flatness deviation of Cubic Molds on Concrete Compressive Strength Results (pre-print)